Joint Centre for Mesoscale Meteorology, Reading, UK

Use of wind-shear displays for Doppler radar data

K. A. Browning
D. Chapman

Internal Report No. 87

May 1998

Met Office Joint Centre for Mesoscale Meteorology Department of Meteorology
University of Reading PO Box 243 Reading RG6 6BB United Kingdom
Tel: +44 (0)118 931 8425 Fax: +44 (0)118 931 8791
www.metoffice.com

Designed and produced by the Met Office © Crown copyright 2001 01/0240 The Met Office logo is a registered trademark.

Use of wind-shear displays for Doppler radar data

D. Chapman and K. A. Browning*

May 28, 1998

* *Corresponding author*: Joint Centre for Mesoscale Meteorology, Department of Meteorology, University of Reading, Whiteknights Road, PO Box 243, Reading, Berkshire, RG6 6BB, UK.

Abstract

The usefulness of displaying vertical wind shear on a radar range height indicator is demonstrated. Fine structure in the pattern of shear is shown to be helpful for inferring general flow patterns and the occurrence of billows due to shearing instability.

1 Introduction

RHIs (Range Height Indicators) of Doppler radar data are usually visualised using colour shading to represent velocity. Although in general this clearly shows extrema in the data, it is very difficult to judge the magnitude of the velocity gradient in either the horizontal or the vertical, and it is even harder to tell if there is a pattern in this gradient field. In this paper we show that, when combined with the original Doppler velocity field, RHIs showing the vertical derivative of the Doppler velocity reveal dynamical processes that would otherwise remain hidden.

Horizontal derivatives giving, for example, horizontal deformation and divergence, are often displayed in the form of RHIs and time-height plots of Doppler radar data. However, there have been few publications showing RHIs of the vertical derivative of the Doppler velocity (vertical shear). The few known to the authors have all been related to observations of Kelvin-Helmholtz (KH) billows. Starr and Browning (1972) showed the numerical values of the vertical shear calculated over 200 m height increments within billows which had a crest-trough amplitude of around 600 m. Browning *et al.* (1973a) showed the vertical shear calculated over 100 m height increments through billows which had a crest-trough amplitude of between 230 and 450m. Although both these studies showed that the shear had maxima in the billows themselves, the resolution of the measurements (compared to the amplitude of the billows) was insufficient to resolve details in the patterns of shear. Recently Chapman and Browning (1997) showed the shear calculated over height increments much smaller than the amplitude of the billows through which the measurements were made. These shear RHIs, obtained within frontal precipitation, show cats-eye

and braided patterns that are very similar to the clear-air reflectivity "signatures" of Kelvin-Helmholtz (KH) billows (see, for examples, the review by Gossard 1990).

James and Browning (1981) showed time-height sections of vertical shear, calculated from high-resolution radar observations made at a fixed elevation angle of 60°, through the upper half of a train of billows. Although in retrospect the patterns seen by Chapman and Browning (1997) can be seen in their data, at the time the structures were not noted, perhaps because observations were not available over the whole depth of the billows. Brown and Rogers (1997) noted multiple shear layers in wind profiler data, possibly associated with gravity waves. However, the resolution of wind profiler data is insufficient to resolve structure due to KH billows, which is the main subject of this paper.

The data that we have examined have all come from the 3 GHz multi-parameter radar (Goddard *et al.* 1994) at Chilbolton (51.15°N, 1.44°W) which is approximately 80 km north of the south coast of England. It has a range resolution of 300 m, and an angular resolution of 0.28°. Although the angular resolution of this radar is unusually high, the success of the method we have used to identify patterns in the wind shear does not depend upon this. In fact, some of our results (not shown here) come from data at ranges of over 100 km, where the resolution is effectively similar to that which would be obtained from a lower-resolution radar at smaller ranges.

When the radar scans with a zero elevation angle the Doppler velocity gives the horizontal component of the wind resolved along the azimuth of the radar beam. At non-zero elevation angles, this horizontal component is contaminated by the vertical fall-speed of the targets (rain or snow in the studies presented here). In addition, as the elevation angle increases, the radar is able to detect a decreasing component of the horizontal velocity. However, for small elevation angles (less than around 10°) these errors in the measurement of the radial component of the horizontal wind are small enough to be neglected. In fact, if one is interested in the detection of essentially qualitative patterns in the data, they may be neglected even at elevations much greater than 10°.

The term "vertical shear" as used in this paper refers to the vertical derivative of the Doppler velocity, evaluated at constant range. Thus the component of vertical shear in the plane of the RHI, as shown in the figures in this paper, is given by

$$S_{i,j} = \frac{\partial V}{\partial Z} \approx \frac{V_{i,j+1} - V_{i,j-1}}{Z_{i,j+1} - Z_{i,j-1}}$$

where V is the Doppler velocity, Z is the height of the scanned volume, and the subscripts i and j refer to range and elevation angle, respectively. For observations made using Chilbolton radar with an angular resolution of 0.28°, S is evaluated over a vertical distance given by $\Delta Z \approx 10 \times Range$ where the height and range are measure in meters and kilometers, respectively. There is an additional error (appreciable only at large elevations) in the expression for S as for non-zero elevations this includes a component of the horizontal gradient of V. This error could be eliminated, although it would result in a more complex expression for the difference approximation.

The following sections describe cases in which RHIs showing the vertical shear indicate the following:

- streamlines in approximately two-dimensional flow,
- KH billows "signature" which in turn indicates mixing (and also possibly significant turbulence),
- multiple shear layers, associated with frontal zones in the cases described here.

2 Transverse circulation at a cold front

a. Validation of streamlines

Figure 1(a) shows a Doppler velocity RHI (ie a vertical cross-section) perpendicular to a rather two-dimensional cold front in which line convection occurred at the surface front (at range 20 km). The front itself was orientated due south-north, and moved eastwards at around 15 m s^{-1}. This front and its environment has been described by Browning *et al.* (1997) who showed front-relative streamlines, defined (assuming two

dimensional flow, with no divergence into the plane) by

$$\frac{\partial \psi}{\partial z} = \rho u,$$

with the boundary condition $\psi = 0$ at the ground. However, here we have instead integrated downwards using a slightly sloping upper boundary condition, at which $\psi = 0$, as this reduces slightly problems associated with the decrease in density with height. The vertical velocity is given by $\partial \psi / \partial x = -\rho w$. These streamlines indicate that cold air approached the surface front from the west, then ascended and receded to the west. Warm air approached the front from the east, rose at the surface front, then continued to flow to the west, ascending gently over the cold air.

For two-dimensional, inviscid, non-rotational flow in which the background density remains constant with height, the component of vorticity lying in a vertical plane (i.e. $\eta = \partial w / \partial x - \partial u / \partial z$) is conserved following the flow. This is as a result of there being no stretching/compression of vortex tubes into the plane. Thus, for steady flow, the component of vorticity lying in the plane would indicate the orientation of streamlines, as flow would be along contours of the vorticity. For most parts of the flow, except near the line convection, $\partial w / \partial x$ is considerably smaller than $\partial u / \partial z$, so the vertical shear on its own will give a good indication of the orientation of the streamlines.

Figure 1(b) shows positive values of the vertical shear, with the streamlines superimposed. Although there is some deformation at the front, resulting in non-conservation of the component of vorticity in the plane, this is fairly small so the shear layer which extends across the domain, at a height of about 1 km ahead of the surface front and around 4 km behind the front is a good indicator of a streamline just above the frontal zone. There is good agreement between this shear layer and the derived streamlines which lie close to it, indicating that the assumptions used in the derivation of the streamline were justified. In other cases where appropriate boundary conditions (perhaps due to lack of data near the ground) cannot be imposed, a shear layer such as this could be used to define a streamline, and the remaining streamlines could be obtained by integration away from it.

b. Shear structures

Chapman and Browning (1997) showed that the shear within large-amplitude billows that were clearly visible in the Doppler returns from frontal precipitation had a cats-eye structure which was similar to the clear-air reflectivity patterns observed by, for example, Browning (1971). Figure 1(c) shows similar patterns in the negative values of the shear between ranges 40 and 60 km at a height of 2 km. The pattern can still be clearly seen in a similar location relative to the front in a number of other RHIs at different times. It has a crest-to-trough amplitude of 1 km and a wavelength of around 4 km, so in these terms could be described as a train of large-amplitude billows. However, the intensity of the pattern is sufficiently weak that the velocity perturbation is too small to be detected easily in the original Doppler field.

The most likely cause of the cats-eye structure seems to be KH billows, although it could possibly be due to an interaction between one thin shear layer and a second such layer, just above. Assuming that the pattern in the shear layer is the result of KH billows, the location is such that they would have been mixing within the weakly stratified cold air mass. Thus they are unlikely to have had a significant effect on the thermodynamic structure of the front, although they would have affected the kinematic structure by redistributing the shear layer. To the extent that the front is similar in structure to a density current, KH billows might be expected close to the "head" between the cold and the warm air flows (at range 25 km, height 3 km). However, the lack of any distinct cats-eye structure in this location indicates that large-amplitude KH billows were **not** occurring in this location, so there was less mixing across the front than might be expected from a comparison with models of density currents.

3 Mixing within frontal zones

The main aim of the previous section was to show that features which are clearly visible in RHIs showing the vertical shear may be almost completely invisible in the

original Doppler velocity RHI. This is particularly true for KH billows, which give rise to a characteristic signature in the shear. The following sections use this property of the shear RHI to identify regions containing KH billows and mixing, primarily within sheared frontal zones.

a. Dual upper cold fronts

Figure 2(a) shows a Doppler RHI through a pair of upper cold fronts which over-ran a surface warm front on 5 January 1998. Each upper cold front has a thermally direct circulation associated with it, as indicated by the arrows in the figure. The structure is similar to that described by Browning *et al.* (1973b) (see Fig. 8 of their paper for a schematic diagram of the processes occurring).

Again the Doppler velocity field is smooth, which would seem to imply that mixing is not occurring between the cold and warm air. However, close inspection of the data between ranges 45 and 55 km at a height of around 3 km, does show some weak wave-like perturbations to the velocity field. These perturbations are much clearer in the shear RHI in Fig. 2(b), and appear as braids/cats-eye structures indicating the existence of KH billows inducing mixing over a depth of 1 km at the statically stable interface between the descending cold and dry upper-tropospheric air, and the ascending warm and saturated lower-tropospheric air. Similar structures existed for the next 30 minutes, until this region had moved too far away from the radar for them to be resolvable. Four separate frontal circulations were sampled by the radar during the observation time (two of which are visible in Fig. 2). Shear structures also existed in some of the other interfaces associated with these circulations, though they were less distinct, and data were not available in some regions because of evaporation of the precipitation as it fell through the cold, dry air.

Whilst in the previous case (Fig. 1) mixing occurred primarily within the cold airflow, in this case mixing occurred across a boundary separating air with different thermodynamic properties and origins. This means that the induced mixing is likely to have been of more importance in terms of the effect on thermodynamic profiles. It

is also of potential importance in bringing together different chemical species which may then react influencing the distribution of chemicals in the troposphere.

b. Mixing associated with fronts during FASTEX

The Fronts and Atlantic Storm Track Experiment (FASTEX) (Joly 1997) was carried out during January and February 1997, in which intensive observations were made of storms and fronts as they developed over the Atlantic, some of which then moved over the UK. During this experiment, the Chilbolton radar was scanned frequently. The scans were made using automated scanning sequences, obtaining RHIs and PPIs alternately through the majority of precipitating frontal regions that passed over the radar between the 4 and 25 February. This dataset is likely to give a good indication of the type and frequency of shear features occurring in frontal regions associated with cyclones over the UK during winter.

The data were studied by looking at both the original Doppler data (RHIs and PPIs) and RHIs of the vertical shear. The results are as follows (see table 1):

- The vast majority of data were from the vicinity of fronts, with a clearly defined vertical shear direction over the depth of the front. Those data (from only a few days) that did not show this have been disregarded in the following paragraphs, as their inclusion would only confuse the points made.
- The majority of the RHIs did not show a single vertical layer over which all the shear (and presumably stability) was concentrated. Instead they showed multiple shear layers on vertical scales of around 1 km.
- Although many of these shear layers remained "laminar" (to the resolution of the radar) for much of the observing time, in **every** observation period (normally lasting a few hours) there were some RHIs in which the shear layers showed "structure" to some degree. This structure consisted of distinct shear patterns, which were coherent over a number of scanning volumes. (It has not been possible to estimate the duration of these features from the data available

because the scanning sequences were such that billows would be missed on a large number of occasions, or observed for only part of the time during which they existed within range of the radar. Also, the radar scans were frequently made such that they scanned mainly perpendicular to frontal regions, rather than parallel to them, so were not in the appropriate direction for detection of billows generated as a result of the thermal wind shear in a frontal zone.)

- The shear layers in which this structure was observed were classified according to Fig. 3. In addition, a subjective estimation of the strength and clarity of the structure was made. Under this scheme, the structures in Fig. 2, for example, would be classified as cats-eyes with medium strength/clarity. Table 1 shows that the braids and cats-eyes all had a vertical extent less than or equal to around 1 km. This is true of all observations of KH billows in the atmosphere known to the authors. Billows of 1 km vertical extent appear to be surprisingly abundant in the data compared with still-resolvable billows of, say, half this amplitude
- The majority of occurrences of braids or billows occurred actually **within** frontal zones, and were not merely loosely associated with them, as in the case shown in Fig. 1(c).

Even though this study is preliminary, the results clearly show that frontal zones often contain multiple shear layers, and that these shear layers frequently show evidence of mixing as a result of KH billows. This is in contrast with the way fronts tend to be represented in most numerical weather prediction models, in which a frontal zone will usually be shown as one shear layer over which, in some cases, mixing is not parameterised in the free atmosphere.

4 Conclusions

This paper has demonstrated the utility of looking at RHIs of vertical shear in addition to RHIs of Doppler velocity, especially for the identification of regions containing KH

billows. In fact, it appears that RHIs of the vertical shear may be used to detect KH billows in regions of precipitation in the same way that reflectivity from high-power radars has been used in the past to detect KH billows in the clear-air. This ability to confidently infer the presence or absence of KH billows makes it possible, in principle, to obtain a climatology of billows in regions of precipitation as well as in the clear air.

From the results of the preliminary study presented here, it appears that KH billows occur considerably more often than might be inferred from inspection of Doppler velocity RHIs alone, even in cases where the billows are of large amplitude, up to 1 km in depth. Billows, and other less well-defined shear features presumably associated with billows, occur predominantly in frontal shear zones, where they may have a significant effect on the kinematic, thermodynamic and chemical properties of the atmosphere. The method described here provides a way of estimating these effects, and whether or not they have significance for weather prediction.

Acknowledgements

We are grateful to the Radio Communications Research Unit at Rutherford Appleton Laboratory for access to the Chilbolton radar. Daniel Chapman is supported by a studentship from the Natural Environment Research Council.

References

Brown, W. O. J. and Rogers, R. R. (1997). Gravity wave and wind shear observations on the McGill weather and profiler radars. *Preprints of the 28th Conference on Radar Meteorology*, pages 512–513.

Browning, K. A. (1971). Structure of the atmosphere in the vicinity of large-amplitude Kelvin-Helmholtz billows. *Quart. J. Roy. Meteor. Soc.*, **97**, 283–299.

Browning, K. A., Bryant, G. W., Starr, J. R., and Axford, D. N. (1973a). Air motion within Kelvin-Helmholtz billows determined from simultaneous doppler radar and aircraft measurements. *Quart. J. Roy. Meteor. Soc.*, **99**, 619–638.

Browning, K. A., Hardman, M. E., Harrold, T. W., and Pardoe, C. W. (1973b). The structure of rainbands within a mid-latitude depression. *Quart. J. Roy. Meteor. Soc.*, **99**, 215–231.

Browning, K. A., Roberts, N. M., and Illingworth, A. J. (1997). Mesoscale analysis of the activation of a cold front during cyclogenesis. *Quart. J. Roy. Meteor. Soc.*, **123**, 2349–2375.

Chapman, D. and Browning, K. A. (1997). Radar observations of wind-shear splitting within evolving atmospheric Kelvin-Helmholtz billows. *Quart. J. Roy. Meteor. Soc.*, **123**, 1433–1439.

Goddard, J. W. F., Eastment, J. D., and Thurai, M. (1994). The Chilbolton advanced meteorological radar: A tool for multidisciplinary research. *Electronics and Communications Engineering Journal*, **6**, 77–86.

Gossard (1990). Radar research on the Atmospheric Boundary Layer. Chapter 27a in *Radar in Meteorology*. Ed. D. Atlas. American Meteorological Society, pages 477–527.

James, P. K. and Browning, K. A. (1981). An observational study of primary and secondary billows in the free atmosphere. *Quart. J. Roy. Meteor. Soc.*, **107**, 351–365.

Joly, A. *et al.* (1997). The fronts and Atlantic storm-track experiment (FASTEX): Scientific objectives and experimental design. *Bull. Amer. Met. Soc.*, **78**, 1917–1940.

Starr, J. R. and Browning, K. A. (1972). Doppler radar measurements of clear air turbulence. *Preprints of the 15th Conference on Radar Meteorology*, pages 248–251.

Date	Obs. Times	Br	C-E	Depth	Synoptic situation
4	1000-1023	-		-	Ahead of SCF, behind SWF
4	2300-2330	s	-	0.5	Above SCF
7	1050-1600	m	w	1.0	Just behind SCF
10	0800-1343	m	w	0.7	Ahead of SCF
11	1200-2010	s	s	1.0	Just ahead of SWF
11	2230-0154	-	-	-	Behind SWF
12	1750-2110	w	-	-	At/behind SCF
13	0030 0330	m	w?	1.0	Behind SCF
14	0845-1349	m	-	0.4	Close to SWF and SCF
17	1830 2230	w	w	0.8	Behind SCF
19	1624-1727	w	-	1.0	At/behind SWF
21	0845-1015	m	-	0.4	Behind SCF/in front of SWF
24	1445-1840	s	m	1.0	Close to SWF and SCF
25	1640-1900	m	w	1.0	Behind SCF

Table 1: The occurrences of braids (Br) and cats-eyes (C-E) (as indicated in Fig. 3) within shear layers in the vertical derivative of Doppler data from Chilbolton radar during February 1997. The times relate to the period of observation, not to the duration of the features (most were only observed for a short time relative to the total observation period). The letters w, m and s (weak, medium and strong, respectively) refer to a subjective estimation of the strength/clarity of the relevant feature. The depth (in km) refers to the approximate vertical extent of the feature/shear layer. The synoptic situation relates to the time at which the "most interesting" features occurred.

List of Figures

1 Data from Chilbolton radar at 1844 UTC on 24 October 1995 at an azimuth of 270°. Note that west is to the left of these plots. (a): Doppler velocity, V (m s^{-1}). (b) Positive values of vertical shear, $\partial V/\partial z$ (m s^{-1} km^{-1}), as defined in the text. (c) Negative values of vertical shear. A mass weighted streamfunction (intervals of 4 kg m^{-2} s^{-1} km) derived from the Doppler velocity data has been used to overlay (a) and (b). 14

2 Data from Chilbolton radar at 1118 UTC on 5 January 1998 at an azimuth of 47°. (a): Doppler velocity, V (m s^{-1}) (b) Vertical shear, $\partial V/\partial z$ (m s^{-1} km^{-1}). 15

3 Classification of the structures observed frequently within vertical shear RHIs. The lines show the patterns of maximum shear. Braids, cats-eyes and a turbulent layer are represented in (a)-(c), respectively. 15

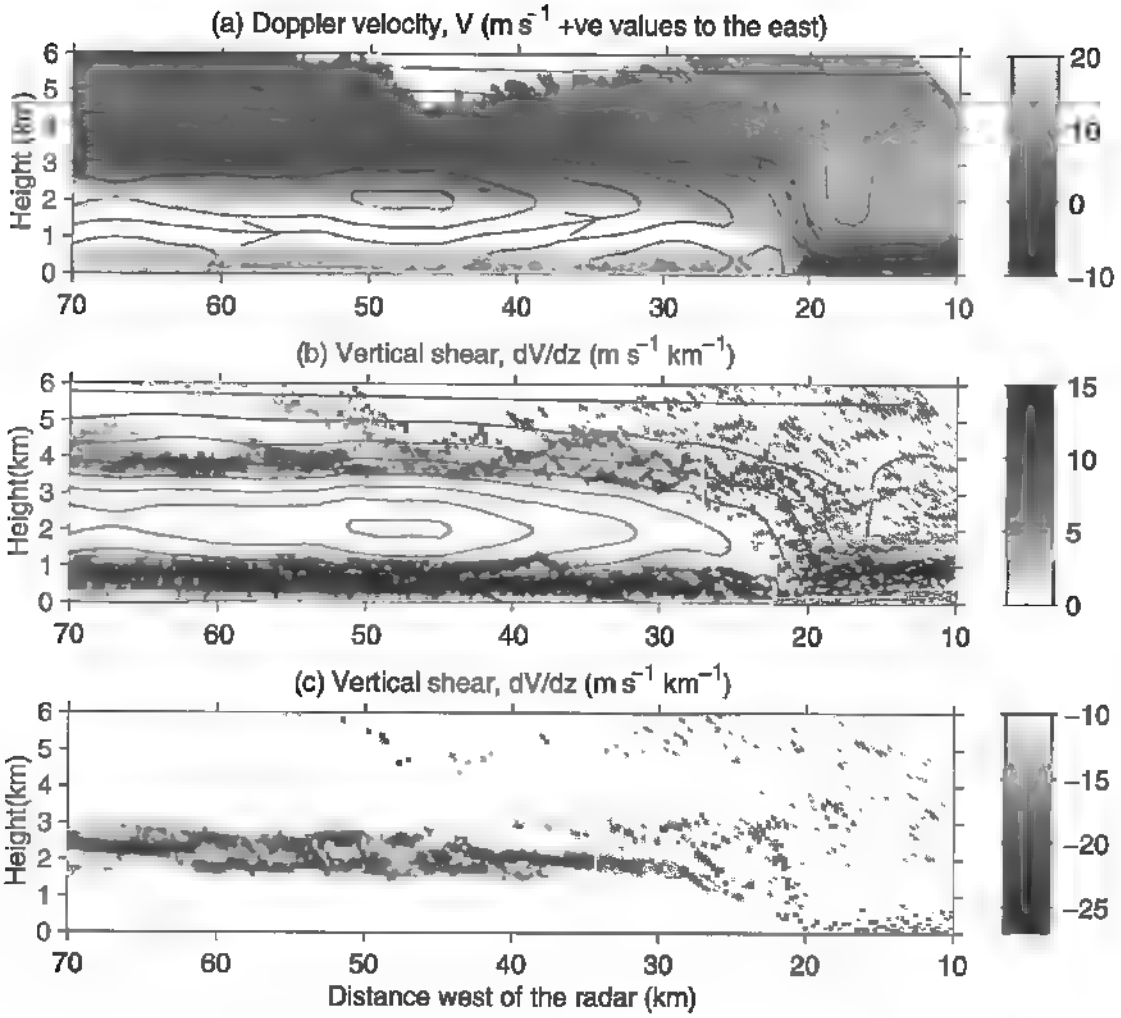

Figure 1: Data from Chilbolton radar at 1844 UTC on 24 October 1995 at an azimuth of 270°. Note that west is to the left of these plots. (a): Doppler velocity, V (m s^{-1}). (b) Positive values of vertical shear, $\partial V/\partial z$ (m s^{-1} km^{-1}), as defined in the text. (c) Negative values of vertical shear. A mass-weighted streamfunction (intervals of 4 kg m^{-2} s^{-1} km) derived from the Doppler velocity data has been used to overlay (a) and (b).

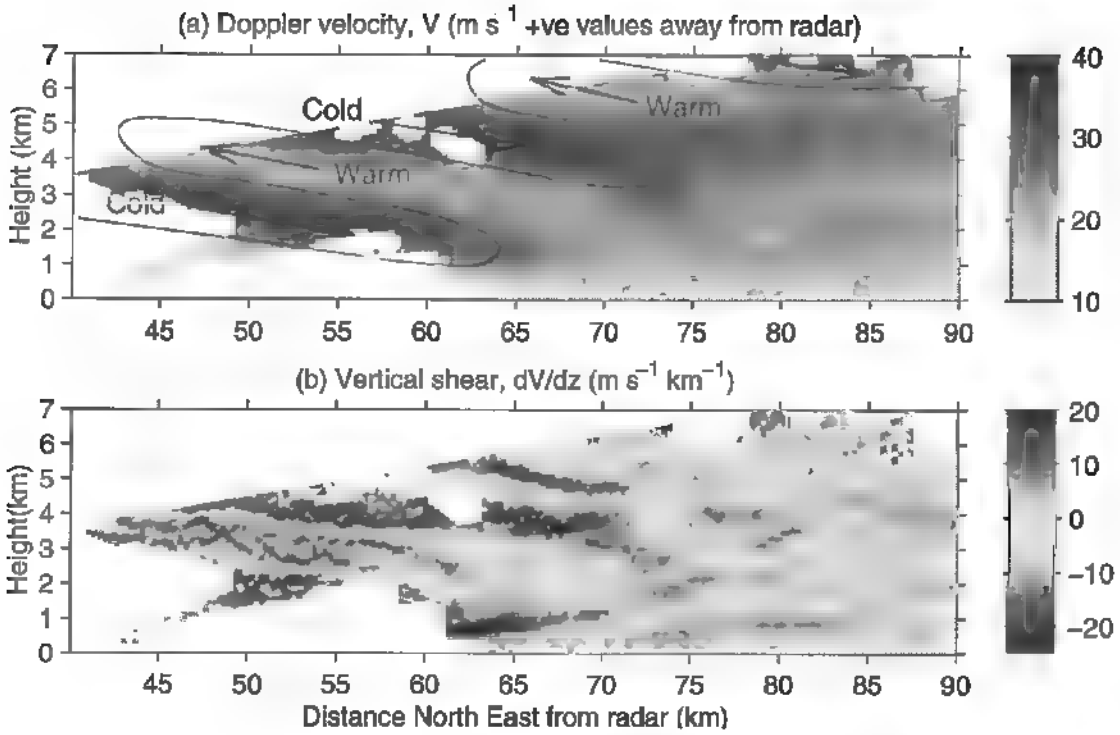

Figure 2: Data from Chilbolton radar at 1118 UTC on 5 January 1998 at an azimuth of 47° (a): Doppler velocity, V (m s^{-1}). (b) Vertical shear, $\partial V/\partial z$ (m s^{-1} km^{-1}).

Figure 3: Classification of the structures observed frequently within vertical shear RHIs. The lines show the patterns of maximum shear. Braids, cats eyes and a turbulent layer are represented in (a) (c), respectively.

CURRENT JCMM INTERNAL REPORTS

This series of JCMM Internal Reports, initiated in 1993, contains unpublished reports and also versions of articles submitted for publication. The complete set of Internal Reports is available from the National Meteorological Library on loan, if required.

1. **Research Strategy and Programme**
   K A Browning et al
   January 1993

2. **The GEWEX Cloud System Study (GCSS)**
   GEWEX Cloud System Science Team
   January 1993

3. **Evolution of a mesoscale upper tropospheric vorticity maximum and comma cloud from a cloud-free two dimensional potential vorticity anomaly**
   K A Browning
   January 1993

4. **The Global Energy and Water Cycle**
   K A Browning
   July 1993

5. **Structure of a midlatitude cyclone before occlusion**
   K A Browning and N Roberts
   July 1993

6. **Development in Systems and Tools for Weather Forecasting**
   K A Browning and G Szejwach
   July 1993

7. **Diagnostic study of a narrow cold frontal rainband and severe winds associated with a stratospheric intrusion**
   K A Browning and R Reynolds
   August 1993

8. **Survey of perceived priority issues in the parametrizations of cloud-related processes in GCMs**
   K A Browning
   September 1993

9. **The Effect of Rain on Longwave Radiation**
   I Dharssi
   September 1993

10. **Physical Cloud Microprocesses - A Description of the Parametrization used in the Large Eddy Model**
    H Swann
    July 1994

11. **An Appreciation of the Meteorological Research of Ernst Kleinschmidt**
    A J Thorpe
    May 1992

12. **Potential Vorticity of Flow Along the Alps**
    A J Thorpe, H Volkert and Dietrich Heimann
    August 1992

13. **The Representation of Fronts**
    A J Thorpe
    January 1993

14. **A Parametrization Scheme for Symmetric Instability: Test for an Idealised Flow**
C S Chan and A J Thorpe
February 1993

15. **The Fronts 92 Experiment: a Quicklook Atlas**
Edited by T D Hewson
November 1993

16. **Frontal wave stability during moist deformation frontogenesis**
Part 1. Linear wave dynamics
C H Bishop and A J Thorpe
May 1993

17. **Frontal wave stability during moist deformation frontogenesis**
Part 2. The suppression of non-linear wave development
C H Bishop and A J Thorpe
May 1993

18. **Gravity waves in sheared ducts**
C Bishop and A J Thorpe
November 1993

19. **Potential Vorticity and the Electrostatics Analogy: Quasi-Geostrophic Theory**
C Bishop and A J Thorpe
November 1993

20. **Recent Advances in the Measurement of Precipitation by Radar**
A J Illingworth
April 1993

21. **Micro-Physique et Givrage. Cloud Microphysics and Aircraft Icing**
A J Illingworth
May 1993

22. **Differential Phase Measurements of Precipitation**
M Blackman and A J Illingworth
May 1993

23. **Estimation of Effective Radius of Cloud Particles from the Radar Reflectivity**
N I Fox and A J Illingworth
May 1993

24. **A Simple Method of Dopplerising a Pulsed Magnetron Radar**
A Hau, A J Illingworth and J Eastment
November 1993

25. **Radiation and Polar Lows**
George C Craig
February 1994

26. **Collected preprints submitted to the International Symposium on the Life Cycles of Extratropical Cyclones; Bergen, Norway, 27 June - 1 July 1994**
April 1994

27. **Convective Frontogenesis**
Douglas J Parker and Alan J Thorpe
April 1994

28. **Improved Measurement of the Ice Water Content in Cirrus Using a Total Water Evaporator**
Philip R A Brown and Peter N Francis
April 1994

29. **Mesoscale Effects of a Dry Intrusion within a Vigorous Cyclone**
K A Browning and B W Golding
April 1994

30. **GEWEX Cloud System Study, Science Plan**
May 1994

31. **Parametrization of Momentum Transport by Convectively Generated Gravity Waves**
R Kershaw
February 1995

32. **Mesoscale Modelling Newsletter No 5**
May 1994

33. **Observations of the mesoscale sub-structure in the cold air of a developing frontal cyclone**
K A Browning, S A Clough, C S A Davitt, N M Roberts and T D Hewson
May 1994

34 **Longwave Radiative Forcing of a Simulated Tropical Squall Line**
Imtiaz Dharssi
July 1994

35. **On the nature of the convective circulation at a kata-cold front**
K A Browning
September 1994

36. **Collective preprints of papers submitted to the COST-75 International Seminar on Advanced Weather Radar Systems, Brussels, 20-23 September 1994**
November 1994

37. **Use of satellite imagery to diagnose events leading to frontal thunderstorms: Parts 1 and 11 of a case study**
K A Browning and N M Roberts
November 1994

38. **The role of spaceborne millimetre-wave radar in the global monitoring of ice cloud**
P R A Brown, A J Illingworth, A J Heymsfield, G M McFarquahar, K A Browning and M Gosset
December 1994

39. **Potential Vorticity Inversion**
Michael Ziemianski
October 1994

40. **Theory of mature tropical cyclones; a comparison between Kleinschmidt (1951) and Emanuel (1986)**
Suzanne L Gray
December 1994

41. **Dispersion and removal of pollutants during the passage of an atmospheric frontal system**
N R Gimson
December 1994

42. **The role of snow sublimation in frontogenesis**
D J Parker and A J Thorpe
December 1994

43. **Potential vorticity and the electrostatics Analogy: Ertel-Rossby formulation**
A J Thorpe and C H Bishop
December 1994

44. **Mesoscale aspect of extratropical cyclones: an observational perspective**
K A Browning
January 1995

45. **A Polar Low Outbreak: Evolution and Mesoscale Structures**
T D Hewson, G C Craig and C Claud
February 1995

46. **Generation of near-surface gusts of deep convection**
K Nakamura and R Kershaw
April 1995

47. **Attribution Concepts applied to the Omega Equation**
S A Clough, C S A Davitt and A J Thorpe
June 1995

48. **Parametrization of mixed-phase cloud and precipitation**
Susan P Ballard and M Gerard Hutchinson
June 1995

49. **Short-range forecasting of stratocumulus: Initialization Prediction**
Susan Ballard, Simon D Jackson and B Macpherson
June 1995

50. **Contributions of the JCMM/Dept of Meteorology Radar Group to the 27th AMS Radar Meteorology Conference, Vail October 1995**
June 1995

51. **Cold Pools in Shear**
Douglas J Parker
September 1995

52. **High-resolution analysis of frontal fracture**
K A Browning, S P Ballard and C S A Davitt
September 1995

53. **The Albedo of Broken Cloud Fields: Calculations using a modified two stream radiation code**
Imtiaz Dharssi and Roy Kershaw
October 1995

54. **Parametrization of momentum transport by convection. I: Theory and cloud modelling results**
R Kershaw and D Gregory
November 1995

55. **Variation of frontal structure along a cold front**
K A Browning and N M Roberts
November 1995

56. **Secondary Frontal Waves**
Douglas Parker
December 1995

57. **Objective Fronts**
T D Hewson
March 1996

58. **Mesoscale analysis of the activation of a cold front during cyclogenesis**
K A Browning, N M Roberts and A J Illingworth
June 1996

59. **Investigation of Different Representations of Rain in a 1-d Evaporation Model**
H Swann
May 1996

60. **Parametrization of diabatic processes in the inversion of the omega-equation**
M Athanassiadou and A J Thorpe
June 1996

61. **The Role of the Environmental Flow in the Development of Secondary Frontal Cyclones**
I A Renfrew, A J Thorpe and A Joly
June 1996

62. **Consequences of the geostrophic momentum approximation on barotropic instability**
S Malardel, A J Thorpe and A Joly
June 1996

63. **Contributions to the AMS/RMS Conference on Mesoscale Processes**
Reading, 9-13 September 1996

64. **Vorticity and Potential Vorticity in Stratified Flows Interacting with an Isolated Obstacle**
Jorge A Gutiérrez and A J Thorpe
September 1996

65. **Triple Point Development: Two Case Studies**
Douglas Parker
September 1996

66. **Radar observations of wind-shear splitting within evolving atmospheric Kelvin-Helmholtz billows**
D Chapman and K A Browning
April 1997

67. **Cold Frontal Structure derived from radar wind profilers**
K A Browning, D Jerrett, J Nash, T Oakley, N M Roberts
May 1997

68. **The dry intrusion and its effect on the frontal, cloud and precipitation structure of extratropical cyclones**
K A Browning - Text of invited special lecture at the Spring Conference
of the Meteorological Society of Japan, University of Tsukuba, 22 May 1997

69. **Met. Office Unified Model data, diagnostic graphics programs, and other observational data available from the JCMM through the aegis of the Universities Weather Research Network (UWERN).** (Plus supplement)
Peter Panagi and Ed Dicks
June 1997

70. **Contributions of the JCMM/Dept of Meteorology Radar Group to 28th AMS Radar Meteorology Conference.** Austin, Texas
September 1997

71. **Sensitivity of short-range weather forecasts to local potential vorticity modifications**
Meral Demirtas and Alan Thorpe
July 1997

72. **Objective identification of frontal wave cyclones**
T D Hewson
August 1997

73. **Attribution and its application to mesoscale structure associated with tropopause folds**
A J Thorpe
September 1997

74. **The Role of the Environmental Flow in the Development of Secondary Frontal Cyclones**
Ian A Renfrew, Alan J Thorpe and Craig H Bishop
September 1997

75. **Potential Vorticity: A short history of its definitions and uses**
Alan J Thorpe and Hans Volkert
September 1997

76. **Superposing Semi-Geostrophic Potential Vorticity Anomalies**
H R Birkett and A J Thorpe
September 1997

77. **Short period forecasting of catchment-scale precipitation.**
Part 1: the role of Numerical Weather Prediction
M A Pedder, M Haile and A J Thorpe
September 1997

78. **Verification of the Tracking Technique Used in an Experimental Cloud Motion Wind Inferring System**
Z Wang, K A Browning and G A Kelly
October 1997

79. **A Preliminary Study of Fourier Series Analysis for Cloud Tracking with GOES High Temporal Resolution Images**
Z Wang
October 1997

80. **Analysis of an ex-tropical cyclone after reintensifying as a warm-core extratropical cyclone**
K A Browning, G Vaughan and P Panagi
November 1997

81. **A JCMM overview of FASTEX IOPs**
S A Clough, H W Lean, N M Roberts, H Birkett, J-P Chaboureau, R Dixon, M Griffiths, T D Hewson and A Montani
January 1998

82. **Programs for PV Inversion and Modification**
Meral Demirtas
December 1997

83. **Release of potential shearing instability in warm frontal zones**
D Chapman and K A Browning
February 1998

84. **The European Cloud-Resolving Modelling Programme (EUCREM)**
Summary Report from the coordinator
P W White
April 1998

85. **A Frontal Wave Database**
T D Hewson
April 1998

86. **Layering Observed in Dropsoundings from IOP 1 of Fronts 92**
S A Clough
May 1998

87. **Use of wind-shear displays for Doppler radar data**
D Chapman and K A Browning
May 1998

Met Office Joint Centre for Mesoscale Meteorology Department of Meteorology
University of Reading PO Box 243 Reading RG6 6BB United Kingdom
Tel: +44 (0)118 931 8425 Fax: +44 (0)118 931 8791
www.metoffice.com